Choosing the best magnetostrictive material for energy harvesting applications: A simple criterion based on Ericsson cycles

Laurent Daniel, Benjamin Ducharne, Yuanyuan Liu, Gael Sebald

Choosing the best magnetostrictive material for energy harvesting applications: a simple criterion based on Ericsson cycles

Laurent Daniel[a,b], Benjamin Ducharne[c,d], Yuanyuan Liu[c,d], Gael Sebald[d]

[a] *Université Paris-Saclay, CentraleSupélec, CNRS, Laboratoire de Génie Electrique et Electronique de Paris, 91192, Gif-sur-Yvette, France*
[b] *Sorbonne Université, CNRS, Laboratoire de Génie Electrique et Electronique de Paris, 75252, Paris, France*
[c] *Univ. Lyon, INSA Lyon, LGEF EA682, Villeurbanne, France*
[d] *ELyTMaX IRL3757, CNRS, Univ Lyon, INSA Lyon, Centrale Lyon, Université Claude Bernard Lyon 1, Tohoku University, Sendai, Japan*

Abstract

The best magnetostrictive material for energy harvesting applications is not necessarily the material with the highest magnetostriction strain. In this paper, based on the description of the Ericsson cycle, a simple criterion to define the most efficient material is proposed. The criterion takes into account the accessible range of stress and magnetic field. It relies on four material parameters only, namely the initial magnetic susceptibility, the saturation magnetisation, the maximum magnetostriction strain and the coercive field of the considered magnetostrictive material. Mass density and price are also involved if a weight optimisation or a cost optimisation is sought. The potential of several materials is compared based on this approach, and it is shown that Giant Magnetostrictive Materials are not systematically the best choice for energy harvesting applications, challenged for some operating conditions by electrical steels.

Keywords: Energy harvesting, magnetostriction, Ericsson cycle, analytical criterion, ultimate harvestable energy.

1. Introduction

Energy harvesting (power harvesting or energy scavenging) is the process of capturing energy from a system's environment and converting it into usable electrical power [1]. One driving force behind the search for new energy-harvesting devices is the desire to power sensor networks and mobile devices without batteries requiring external charging or service. This statement is especially valid in the rapidly growing field of the Internet of Things (IoTs) [2, 3]. Various energy sources, such as wind, solar, geothermal, hydropower, or vibration can be considered. All these methods have pros and cons, but the needs for alternative energy are so significant that none of them can really be left apart from scientific investigations.

This work focuses on vibration. It has many advantages, such as availability, energy levels in the range of IoTs needs, and ubiquity [4, 5]. Here, energy is scavenged from ambient mechanical vibrations of multiple origins (vehicles, machinery, etc) and physical characteristics (with frequencies from 0.1 Hz to 1 kHz and accelerations from 0.01 to 1 g) [6].

Due to the extensive range of vibration properties, various designs of harvesters have been described in the scientific literature [7, 8, 9]. Vibration energy harvesters can be classified as electromagnetic or electrostatic when no active conversion occurs. In that case, the vibration source induces a relative motion between coils and permanent magnets (electromagnetic [10]) or movable electrodes (electrostatic [11]). Oppositely, active energy harvesters use functional materials (mainly piezoelectric [12] or magnetostrictive [6]) that convert mechanical energy into a magnetic or electrical energy form. Piezoelectric materials show a high coupling coefficient but are brittle, can be depolarised, and exhibit high output impedances [6]. Regarding these aspects, magnetostrictive materials are much more adapted even if they also show limitations like their highly nonlinear behavior [6].

Comparing the performance of magnetostrictive materials in the energy harvesting context is mandatory for designing optimal harvesters. It raises many questions:

- Is the best material necessarily the one with the highest magnetostriction coefficient?
- Are there any optimal loading conditions?

◦ Is a bias magnetic field required to improve the conversion efficiency?
◦ What would be the ultimate amount of energy converted? And what are the parameters driving this value?

Multiple experimental results are available in the scientific literature, but the working conditions are always different, making such comparisons impossible. Alternatively, this study proposes a simple analytical expression to predict the level of magnetostrictive conversion and to answer these questions. The model constitutes a decision tool for a given loading condition regarding volume, weight, or price optimisation. 3D stress configurations are considered, and the approach requires only four material parameters, easily found in the literature: the magnetisation saturation M_s, the maximum magnetostriction strain λ_s, the maximum permeability χ^o and the coercive field H_c (replaced by an applied bias field H_b if relevant).

This study is intended to assess the energy conversion capability of magnetostrictive materials, therefore, no specific device or electrical interface will be considered. The investigation is restricted to the pure magneto-mechanical conversion. The design of magnetic circuits, coils, and associated instrumentation will not be discussed.

The paper is organised as follows: The thermodynamic Ericsson cycles used to assess the mechano-magnetic conversion are introduced first. The analytical model to define the proposed criterion is then described. A comparison between different materials available for energy harvesting applications is finally proposed, followed by a general conclusion.

2. The Ericsson cycle as a mean to assess energy harvesting capabilities

Thermodynamic cycles are required to evaluate the converted energy appropriately [13]. In this work, we opt for the magnetostrictive Ericsson cycle as an image of energy conversion capability. The Ericsson cycle consists of two branches at constant mechanical stress and two others at constant magnetic field (see Fig. 1 for illustration and [13, 14] for additional explanations about Ericsson cycles). Considering a magnetostrictive specimen, the Ericsson cycle is covered in four steps shown in Fig. 1, starting from state 1 with no applied magnetic field ($\mathbf{H} = \mathbf{0}$) and a stress state $\boldsymbol{\sigma} = \boldsymbol{\sigma}_1$:

◦ Stage 1 to 2: the magnetic field $\mathbf{H}$ is kept at $\mathbf{0}$ and the stress $\boldsymbol{\sigma}$ is changed from $\boldsymbol{\sigma}_1$ to $\boldsymbol{\sigma}_2$.
◦ stage 2 to 3: the stress $\boldsymbol{\sigma}$ is kept at $\boldsymbol{\sigma}_2$ and the magnetic field $\mathbf{H}$ is changed from $\mathbf{0}$ to $\mathbf{H}_{\max}$.
◦ stage 3 to 4: the magnetic field $\mathbf{H}$ is kept at $\mathbf{H}_{\max}$ and the stress $\boldsymbol{\sigma}$ is changed from $\boldsymbol{\sigma}_2$ to $\boldsymbol{\sigma}_1$.
◦ stage 4 to 1: the stress $\boldsymbol{\sigma}$ is kept at $\boldsymbol{\sigma}_1$ and the magnetic field $\mathbf{H}$ is changed from $\mathbf{H}_{\max}$ back to $\mathbf{0}$.

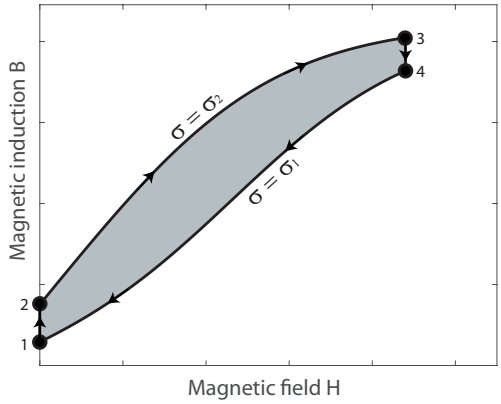

Figure 1: Ericsson cycle

The resulting loop area (grey zone in Fig. 1) in the $B(H)$ plane (where B is the magnetic flux density) can be considered an image of the ultimate magneto-elastic energy conversion capability of the material. In that sense, whatever the electrical interface, the converted energy will not be higher than the Ericsson cycle area. This area can therefore be considered an indicator of the conversion capability, and different materials can be compared accordingly. The approach is meant as a general assessment of the energy harvesting potential of magnetostrictive materials, but the possibility to use practically the Ericsson cycle as a mean of energy harvesting is discussed in Appendix A.

3. Simplified calculation of the Ericsson energy area

The purpose of this section is to provide an analytical expression for the Ericsson cycle area, based on an analytical definition of the anhysteretic magnetisation curve.

3.1. Analytical definition of the magnetisation curve

The works in [15] provide an analytical expression for the stress-dependant anhysteretic magnetisation curve of ferromagnetic materials. The magnetisation $\mathbf{M}$ is expressed as:

$$\mathbf{M} = \frac{A_x \sinh(\kappa H)}{A_x \cosh(\kappa H) + A_y + A_z} M_s \mathbf{x}, \tag{1}$$

where H is the amplitude of the magnetic field $\mathbf{H}$ applied along direction $\mathbf{x}$ ($\mathbf{H} = H\,\mathbf{x}$). The coefficients A_x, A_y and A_y are functions of the applied stress $\boldsymbol{\sigma}$:

$$A_x = \exp(\alpha\,\sigma_{xx}); \quad A_y = \exp(\alpha\,\sigma_{yy}); \quad A_z = \exp(\alpha\,\sigma_{zz}) \tag{2}$$

where σ_{xx} (resp. σ_{yy}, σ_{zz}) is the principal component of the stress tensor $\boldsymbol{\sigma}$ along direction $\mathbf{x}$ (resp. $\mathbf{y}$, $\mathbf{z}$). The expression (1) introduces three material parameters M_s, κ and α. M_s is the saturation magnetisation of the material. It was shown in [15] that κ and α can be connected to standard material parameters according to (3).

$$\kappa = \frac{3\chi^o}{M_s} \qquad \text{and} \qquad \alpha = \frac{9\,\lambda_s \chi^o}{2\,\mu_0\,M_s} \tag{3}$$

χ^o is the initial (at no applied field) anhysteretic susceptibility of the material under stress-free conditions. It can reasonnably be approximated by the maximum stress-free magnetic relative permeability of the material. λ_s is the maximum magnetostriction strain of the material, and μ_0 is the vacuum permeability.

Using these relations the anhysteretic stress-dependent magnetisation curve of a material can be defined using only three standard material parameters: the saturation magnetisation M_s, the maximum magnetostriction λ_s and the maximum magnetic susceptibility (or relative magnetic permeability) χ^o.

Due to the very strong assumptions made to obtain such a simple expression [15], the model may struggle in some cases to describe quantitatively the magnetisation for a given magneto-elastic loading ($\mathbf{H}$, $\boldsymbol{\sigma}$). However the model was shown to predict the correct trends for the magneto-elastic behaviour (see for instance [16]). Moreover, in the following, the model will be integrated over large spans of magnetic field, which tends to compensate for local inaccuracies.

3.2. Analytical definition of the Ericsson energy area

We now consider two anhysteretic magnetisation curves of a given material. A first curve under a stress state $\boldsymbol{\sigma}_1$, and a second curve under a stress state $\boldsymbol{\sigma}_2$. The area $A_v(H_m, \boldsymbol{\sigma}_1, \boldsymbol{\sigma}_2)$ of the corresponding Ericsson cycle for a maximum field H_m is simply given by (4) in which we assume that $\boldsymbol{\sigma}_1$ and $\boldsymbol{\sigma}_2$ have been ordered so that $A_v(H_m, \boldsymbol{\sigma}_1, \boldsymbol{\sigma}_2) > 0$ (otherwise an absolute value can be added to (4)).

$$A_v(H_m, \boldsymbol{\sigma}_1, \boldsymbol{\sigma}_2) = \int_{H_b}^{H_b+H_m} \left(B(H_m, \boldsymbol{\sigma}_2) - B(H_m, \boldsymbol{\sigma}_1)\right)\, dH \tag{4}$$

H_b is a magnetic field, larger than the coercive field, that can be applied to consider a bias field and/or the hysteresis loss in the harvested energy calculus. In the case no bias-field is applied, the value of H_b is taken as the coercive field H_c. Using the expression of the stress-dependent anhysteretic magnetisation curve (1), the development of (4) yields the fully analytical expression (5) for the area of the Ericsson cycle in the general 3D-case.

$$A_v(H_m, \boldsymbol{\sigma}_1, \boldsymbol{\sigma}_2) = \frac{\mu_0\,M_s}{\kappa} \ln\left(\frac{A_x(\boldsymbol{\sigma}_2)\cosh(\kappa\,(H_b + H_m)) + A_y(\boldsymbol{\sigma}_2) + A_z(\boldsymbol{\sigma}_2)}{A_x(\boldsymbol{\sigma}_1)\cosh(\kappa\,(H_b + H_m)) + A_y(\boldsymbol{\sigma}_1) + A_z(\boldsymbol{\sigma}_1)} \times \frac{A_x(\boldsymbol{\sigma}_1)\cosh(\kappa\,H_b) + A_y(\boldsymbol{\sigma}_1) + A_z(\boldsymbol{\sigma}_1)}{A_x(\boldsymbol{\sigma}_2)\cosh(\kappa\,H_b) + A_y(\boldsymbol{\sigma}_2) + A_z(\boldsymbol{\sigma}_2)}\right) \tag{5}$$

.

This expression gives the area of the Ericsson cycle in terms of Energy per volume unit. It can also be useful to describe the potential of a material in terms of energy per mass unit or in terms of energy per price unit. The corresponding expressions $A_m(H_m, \boldsymbol{\sigma}_1, \boldsymbol{\sigma}_2)$ and $A_\$(H_m, \boldsymbol{\sigma}_1, \boldsymbol{\sigma}_2)$ are given by (6), where ρ is the mass density of the material and $p_\$$ its price per mass unit.

$$A_m(H_m, \boldsymbol{\sigma}_1, \boldsymbol{\sigma}_2) = \frac{1}{\rho} A_v(H_m, \boldsymbol{\sigma}_1, \boldsymbol{\sigma}_2) \quad \text{and} \quad A_\$(H_m, \boldsymbol{\sigma}_1, \boldsymbol{\sigma}_2) = \frac{1}{p_\$} A_m(H_m, \boldsymbol{\sigma}_1, \boldsymbol{\sigma}_2) = \frac{1}{\rho\, p_\$} A_v(H_m, \boldsymbol{\sigma}_1, \boldsymbol{\sigma}_2) \tag{6}$$

3.3. Simplification in the case of uniaxial stress applied along the field direction

In the case where one of the curves used for the Ericsson cycle is the stress-free magnetisation curve ($\boldsymbol{\sigma}_2 = \mathbf{0}$) and the second is a curve obtained under a uniaxial stress with amplitude σ applied parallel to the applied field ($\boldsymbol{\sigma}_1 = \sigma\, \mathbf{x} \otimes \mathbf{x}$), the area $A_v(H_m, \sigma, 0)$ of the Ericsson cycle simplified into (7)

$$A_v(H_m, \sigma, 0) = \frac{\mu_0\, M_s}{\kappa} \ln\left(\frac{\exp(\alpha\, \sigma) \cosh(\kappa\, H_b) + 2}{\exp(\alpha\, \sigma) \cosh(\kappa\, H_m) + 2} \times \frac{\cosh(\kappa\, H_m) + 2}{\cosh(\kappa\, H_b) + 2} \right) \tag{7}$$

3.4. Ultimate achievable energy conversion under uniaxial stress

Assuming that it is possible to reach any level of magnetic field, it is interesting to see what is, for a given uniaxial stress σ, the ultimate area $A_v(H_\infty, \sigma, 0)$ that can be covered by the Ericsson cycle. The expression (8) is simply obtained by taking the limit of (7) when H_m tends to infinity.

$$A_v(H_\infty, \sigma, 0) = \frac{\mu_0\, M_s}{\kappa} \ln\left(\frac{\cosh(\kappa\, H_b) + 2\, \exp(-\alpha\, \sigma)}{\cosh(\kappa\, H_b) + 2} \right) \tag{8}$$

4. Comparison of different materials for energy harvesting applications

This section is dedicated to the comparison of different materials regarding their potential for energy harvesting applications, based on their respective properties. The tested magnetic materials are listed in Table 1 with their relevant properties, taken from the literature. For the sake of simplicity, and although the proposed analytical approach can assess the potential of a material for any multiaxial loading, the analysis is here restricted to uniaxial loading configurations (uniaxial stress σ applied parallel to the magnetic field H).

4.1. Comparison based on volume efficiency

A first comparison can be made based on the maximum harvestable energy per volume unit. Based on (7), table 2 shows the performance of the tested materials for various uniaxial stress σ (compressive) and various maximum field levels H_m. For each couple (H_m, σ), the better performance is indicated in dark colour and materials still competitive with the best performance are indicated in light colour.

At high levels of magnetic field H_m (of the order of 100 kA.m^{-1}), Giant Magnetostrictive Materials (GMM, Terfenol-D and Galfenol), clearly show the best performance. If low levels of magnetic field H_m are considered, competitors emerge. FeNi and Fe-based amorphous alloys at low stress levels and GO FeSi or Polycrystalline Fe for higher stress levels reveal better capability than GMM in these ranges. This is due to the low magnetic permeability of GMM which requires high levels of applied magnetic field to exploit their full potential.

4.2. Comparison based on weight efficiency

Combining (7) with the left part of (6), the tested materials can be compared based on the maximum harvestable energy per mass unit. Given the small differences in the mass density between the tested materials, such a comparison brings essentially the same results as the comparison based on the maximum harvestable energy per volume unit. Therefore it will not be detailed here.

	M_s	λ_s	$\chi^{o\star}$	H_c	ρ	$p_\$$ [†]	Ref.[‡]
	10^6 A.m^{-1}	10^{-6}	-	A.m^{-1}	kg.m^{-3}	\$.kg^{-1}	
Polycrystalline Iron (Poly Fe)	1.72	5.0	50 000	10	7867	10	[17]
Non-oriented Iron Silicon steel (FeSi NO)	1.69	10	10 000	30	7700	1.2	[17]
Grain-oriented Iron Silicon steel (FeSi GO)	1.61	3.0	80 000	4	7650	1.5	[17]
Permalloy (FeNiMo)	0.64	1.0	500 000	1	8700	30	[17]
Permendur (FeCo-2V)	1.87	60	2 000	30	8200	100	[17]
Fe50-Ni50	1.27	25	100 000	4	8120	40	[17]
Fe-based amorphous alloys (Fe-amorph)	1.24	40	100 000	2	7500	100	[17]
Co-based Amorphous alloys (Co-amorph)	0.49	0.5	500 000	1	7500	100	[17]
Nanocrystalline alloys (Finemet)	0.99	2.0	500 000	1	7200	14	[17]
Nanocrystalline alloys (Nanoperm)	1.21	0.1	50 000	3	7200	14	[17]
Terfenol-D	0.18	700	10	2500	9200*	15000	[18]
Galfenol	0.14	200	20	150	7800*	10000	[19]

Table 1: Choice of magnetostrictive candidates for energy harvesting applications: saturation magnetisation M_s, maximum magnetostriction λ_s, initial anhysteretic susceptibility of the stress-free magnetisation curve χ^o, coercive field H_c, mass density ρ, price $p_\$$. *When not directly available, the maximum magnetic permeability was used. [†]Prices can be subjected to considerable variations based on time and volume. [‡]Except for price, found at various suppliers online. *Mass density for Terfenol-D and Galfenol were obtained from http://tdvib.com.

H_m (A.m^{-1})	10^2	10^3	10^4	10^5	10^2	10^3	10^4	10^5	10^2	10^3	10^4	10^5	10^2	10^3	10^4	10^5
$\lvert\sigma\rvert$ (MPa)	10	10	10	10	25	25	25	25	50	50	50	50	100	100	100	100
Poly Fe	62	63	63	63	154	174	174	174	169	362	362	362	169	737	737	737
FeSi NO	31	114	114	114	52	324	324	324	56	696	696	696	56	1 443	1.4k	1.4k
FeSi GO	39	39	39	39	106	106	106	106	176	219	219	219	177	444	444	444
Permalloy	15	15	15	15	37	37	37	37	75	75	75	75	79	150	150	150
Permendur	7	490	702	702	11	979	2.0k	2.0k	11	1.1k	4.2k	4.2k	11	1.1k	8.7k	8.7k
Fe50-Ni50	147	371	371	371	147	934	934	934	147	1.6k	1.9k	1.9k	147	1.6k	3.7k	3.7k
Fe-amorph	144	597	597	597	144	1.5k	1.5k	1.5k	144	1.5k	3.0k	3.0k	144	1.5k	1.5k	1.5k
Co-amorph	7	7	7	7	19	19	19	19	37	37	37	37	62	75	75	75
Finemet	30	30	30	30	75	75	75	75	123	150	150	150	123	300	300	300
Nanoperm	1	1	1	1	3	3	3	3	5	5	5	5	12	12	12	12
Terfenol-D	39	33	582	9.9k	39	33	582	20.1k	39	33	582	20.1k	39	33	582	20.1k
Galfenol	0	12	1.0k	2.8k	0	12	1.0k	7.3k	0	12	1.0k	14.8k	0	12	1.0k	16.6k

Table 2: Area $A_v(H_m, \sigma, 0))$ of the Ericsson cycle (in μJ.cm^{-3}) for different materials under different loading conditions. Uniaxial stress is compressive ($\sigma < 0$).

4.3. Comparison based on cost efficiency

Combining (7) with the right part of (6), a comparison based on price can be performed. It will reveal the maximum harvestable energy per price unit. The results are given in table 3, showing under the same uniaxial loading conditions as table 2. Again, for each couple (H_m, σ), the better performance is indicated in dark colour and materials still competitive with the best performance are indicated in light colour.

It is evident that the conclusions are very different compared to the case where volume (or weight) is to be optimised. Due to their very high price, GMM are not competitive anymore. Electrical steels on the contrary are produced in huge quantities, resulting in a very low cost, making them very competitive here for energy harvesting applications. Of course, these conclusions can evolve drastically based on price fluctuations, or required material

H_m (A.m^{-1})	10^2	10^3	10^4	10^5	10^2	10^3	10^4	10^5	10^2	10^3	10^4	10^5	10^2	10^3	10^4	10^5
$\|\sigma\|$ (MPa)	10	10	10	10	25	25	25	25	50	50	50	50	100	100	100	100
Poly Fe	792	796	796	796	2.0k	2.2k	2.2k	2.2k	2.1k	4.6k	4.6k	4.6k	2.1k	9.4k	9.4k	9.4k
FeSi NO	3.4k	12.3k	12.3k	12.3k	5.6k	35.1k	35.1k	35.1k	6.1k	75.3k	75.3k	75.3k	6.1k	156k	156k	156k
FeSi GO	3.4k	3.4k	3.4k	3.4k	9.2k	9.3k	9.3k	9.3k	15.4k	19.1k	19.1k	19.1k	15.4k	38.7k	38.7k	38.7k
Permalloy	56	56	56	56	142	142	142	142	286	286	286	286	303	573	573	573
Permendur	9	598	857	857	13	1.2k	2.4k	2.4k	14	1.4k	5.1k	5.1k	14	1.4k	10.6k	10.6k
Fe50-Ni50	452	1.1k	1.1k	1.1k	452	2.9k	2.9k	2.9k	452	4.9k	5.8k	5.8k	452	4.9k	11.5k	11.5k
Fe-amorph	192	796	796	796	192	2.0k	2.0k	2.0k	192	2.1k	4.0k	4.0k	192	2.1k	2.1k	2.1k
Co-amorph	10	10	10	10	25	25	25	25	50	50	50	50	82	100	100	100
Finemet	294	294	294	294	740	740	740	740	1.2k	1.5k	1.5k	1.5k	1.2k	3.0k	3.0k	3.0k
Nanoperm	10	10	10	10	25	25	25	25	53	53	53	53	114	114	114	114
Terfenol-D	<1	<1	4	72	<1	<1	4	146	<1	<1	4	146	<1	<1	4	146
Galfenol	<1	<1	13	36	<1	<1	13	94	<1	<1	13	190	<1	<1	13	213

Table 3: Area $A_\$(H_m, \sigma, 0))$ of the Ericsson cycle (in μJ.\$$^{-1}$) for different materials under different loading conditions. Uniaxial stress is compressive ($\sigma < 0$).

quantity, but the proposed simple analytical formulas (7) and (6) allow for an updated view may price vary or other materials emerge.

4.4. Maximum harvestable energy for a given magneto-mechanical loading

Still considering uniaxial loadings, for the sake of simplicity, it is interesting to look, based on the available material database, at the best achievable harvested energy for a given stress σ and magnetic field H_m. Depending on the couple (H_m, σ), this best achievable harvested energy will be provided by different materials. The space (H_m, σ) for compressive stress has been scanned for all materials in table 1, and the maximum harvestable energy has been picked up for all loading conditions. The results are shown in Fig. 2.

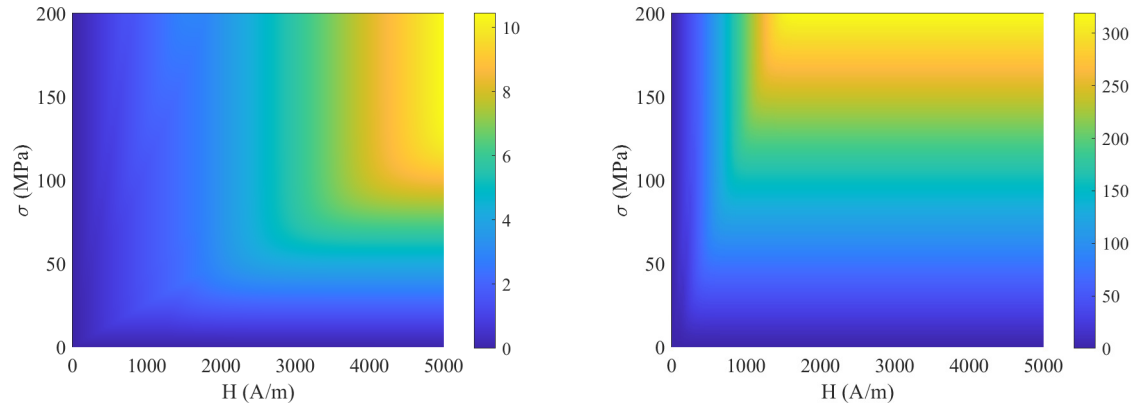

(a) Energy per volume unit (mJ.cm^{-3})

(b) Energy per price unit (mJ.\$$^{-1}$)

Figure 2: Maximum harvestable energy for all tested materials as a function of the loading conditions (uniaxial configuration with compressive stress).

High conversion performance, in terms of volume (and mass), can only be achieved by reaching very high field levels. Such configurations correspond to regions where GMM exhibit very high performance. On the contrary high conversion performance in terms of cost does not require very high levels of magnetic field. This is due to the competitiveness of electrical steels at low magnetic field H_m.

4.5. *Ultimate harvestable energy conversion*

Another comparison that can be made between the different magnetostrictive materials consists in plotting the ultimate achievable energy conversion under uniaxial stress (compression). The results are shown in Fig. 3, for a comparison based on volume (left) and a comparison based on cost (right). It is reminded that a comparison based on the ultimate harvestable energy conversion supposes that the maximum level of magnetic field H_m required to obtained the best performance of a given material is attainable.

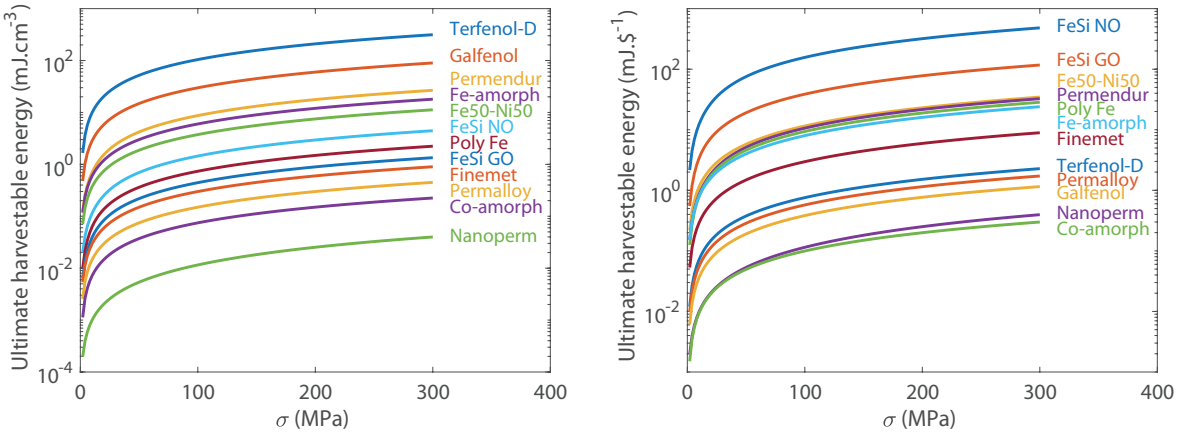

(a) Energy per volume unit (mJ.cm^{-3})

(b) Energy per price unit (mJ.\$$^{-1}$)

Figure 3: Ultimate harvestable energy for all tested materials as a function of the available stress amplitude (uniaxial configuration).

As expected, GMM show the best performance in terms of volume optimisation. In terms of cost optimisation, electrical steels are the best materials. Fig. 3 also shows that some materials are clearly not competitive for energy harvesting applications (e.g. Co-based amorphous alloys, Nanoperm, or Permalloy). This is mostly due to very low magnetostriction λ_s and relatively small M_s. As already highlighted, choosing an optimisation based on volume/weight or cost totally changes the definition of the most efficient material.

5. Conclusion

In this paper, the area of Ericsson cycle under uniaxial magneto-elastic loading was used as an indicator of energy harvesting capabilities of various magnetic materials. An analytical model was developed. The model is based on standard material parameters (saturation magnetisation M_s, maximum magnetostriction λ_s, initial anhysteretic susceptibility of the stress-free magnetisation curve χ^o, coercive field H_c, mass density ρ and price $p_\$$). For configurations when a bias field H_b is used for energy harvesting the coercive field H_c can be replaced by H_b in the obtained formulas. The model was used to compare various with respect to their energy harvesting potential. The comparison was performed for the case of uniaxial magneto-elastic loadings but the model is applicable to multiaxial configurations. It is shown that when optimising volume (or weight) Giant Magnetostrictive materials (Terfenol-D and Galfenol) offer the highest efficiency for energy harvesting if no limitation is given on the amplitude of the magnetic field. However if high values of magnetic field cannot be reached, some iron-based materials appear as challengers. Below magnetic field levels of a few thousands A.m^{-1}, Giant Magnetostrictive Materials are no longer competitive.
Based on price, the game is totally changed and electrical steels appear to be excellent candidates for energy harvesting applications. Of course prices are subject to considerable variations depending on availability and volume, so that the conclusions drawn can be rapidly outdated. But the analytical criterion proposed allows easy and continuous updating. It is also worth noting that the material is not everything in the design of an energy harvesting device, and the volume and cost of the surrounding system also plays a role, which was not discussed in this study.

Appendix A. Applicability of energy harvesting devices based on Ericsson cycles

This article compares the harvesting capability of different magnetostrictive materials based on the Ericsson cycle. In order to support the significance of this theoretical approach, we show in this appendix how the Ericsson cycle can be used as an actual energy harvesting cycle. The objective is notably to show that the harvested energy can significantly exceed the amount required for the cycle creation.

The generation of a real-timely controlled, high-amplitude magnetic excitation is a critical aspect. Permanent magnets used in electromagnetic devices generate magnetic fields of constant amplitude, which is unsuitable in the Ericsson cycle context. Excitation coils are the only alternative option, but to the price of Joule losses. A simple analytical development can be proposed to assess the ratio r between the amount of harvested energy W_{harv} and the amount of energy W_{J} lost by Joule effect in the excitation coil:

$$r = \frac{W_{\text{harv}}}{W_{\text{J}}} \tag{A.1}$$

Based on such analysis, optimized experimental conditions can be given to maximize the ratio r, inspired from the study case in [20]. Consider a rod of magnetostrictive material, with diameter $\Phi = 40$ mm and height $h = 200$ mm (Fig. A.4). The excitation field H_m is tested in the range $[\,0.1\ 100\,]$ kA.m^{-1}, and the maximal current I is imposed to be no larger than 10 A. The coil wire diameter Φ_{w} is set to ensure a temperature elevation lower than 50°C. A first calculus based on (A.2) is done to estimate the height h_{c} of the resulting coil, where N is the number of turns, n_{lay} the number of layers for the coil, and $\rho_{\text{corr}} = 1.1$ a correction coefficient to take into account the wire dielectric coating and some potential irregularities in the turns distribution.

$$h_{\text{c}} = \rho_{\text{corr}} \frac{N\,\Phi_{\text{w}}}{n_{\text{lay}}} \tag{A.2}$$

Several conclusions can be drawn from (A.2):

- n_{lay} has to be larger than 25 to generate $H_m = 100$ kA.m^{-1} while keeping h_{c} lower than h.
- a single layer coil is enough to generate up to $H_m = 1$ kA.m^{-1}
- three layers are the minimal requirement to reach $H_m = 10$ kA.m^{-1}

The Joule losses can then be calculated using (A.3), where R is the in-series coil resistance, and f is the frequency of current waveform, assumed triangular (Fig. A.4).

$$W_{\text{J}} = \frac{R\,I^2}{3f} \tag{A.3}$$

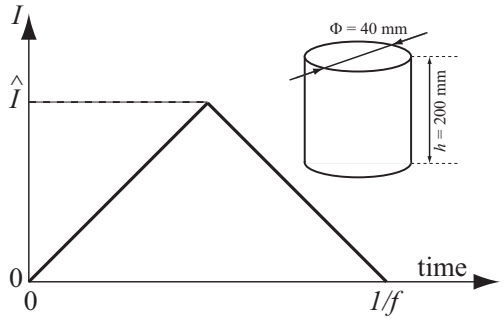

Figure A.4: Rod specimen and electrical current waveform.

On the other hand, W_{harv} is obtained by multiplying the results from Table 2 by the volume of the considered magnetostrictive materials (aprox. 250 cm^3 with the geometry considered here). The calculation of r is limited here to the materials identified in the study as potential candidates for energy harvesting applications:

- FeSi NO and FeSi GO from Table 3 criterion
- Fe-amorph from Table 2 criterion at low magnetic fields
- Terfenol-D from Table 2 criterion at high magnetic fields

The ratio r is presented for the selected materials in Table A.4. The practically of use of an Ericsson cycle is set - arbitrarily - for ratios r above 5 (green-colored cells in Table A.4). In the low field range (H_m = 100 A.m^{-1}), this criterion is met for all materials. Oppositely, only Terfenol-D fulfills this criterion in the high field range. FeSi GO exhibits the largest r (> 60) but only in the low field range where the amount of harvested energy is limited. Of course these results are dependent on the specimen geometry, but provide the trends for material performance.

	I (A)	1	5	10	1	5	10	1	5	10	1	5	10
	H_m (kA.m^{-1})	0.1	0.1	0.1	1	1	1	10	10	10	100	100	100
	N	20	4	2	200	40	20	2000	400	200	20000	4000	2000
-10 MPa	FeSi NO	11.00	10.96	10.92	4.04	4.03	4.01	0.40	0.40	0.40	0.04	0.04	0.04
-10 MPa	FeSi GO	13.83	13.79	13.73	1.38	1.38	1.37	0.14	0.14	0.14	0.01	0.01	0.01
-10 MPa	Fe-amorph	51.08	50.93	50.70	21.18	21.11	21.02	2.12	2.11	2.10	0.21	0.21	0.21
-10 MPa	Terfenol-D	13.83	13.79	13.73	1.14	1.13	1.13	2.07	2.06	2.05	3.51	3.50	3.49
-25 MPa	FeSi NO	18.44	18.39	18.31	1.84	1.84	1.83	0.18	0.18	0.18	0.02	0.02	0.02
-25 MPa	FeSi GO	37.60	37.49	37.32	3.76	3.75	3.73	0.38	0.37	0.37	0.04	0.04	0.04
-25 MPa	Fe-amorph	51.08	50.93	50.70	5.11	5.09	5.07	0.51	0.51	0.51	0.05	0.05	0.05
-25 MPa	Terfenol-D	13.83	13.79	13.73	1.38	1.38	1.37	0.14	0.14	0.14	0.01	0.01	0.01
-50 MPa	FeSi NO	19.86	19.81	19.72	24.69	24.62	24.51	2.47	2.46	2.45	0.25	0.25	0.25
-50 MPa	FeSi GO	62.43	62.25	61.97	7.77	7.75	7.71	0.78	0.77	0.77	0.08	0.08	0.08
-50 MPa	Fe-amorph	51.08	50.93	50.70	53.20	53.05	52.81	10.64	10.61	10.56	1.06	1.06	1.06
-50 MPa	Terfenol-D	13.83	13.79	13.73	1.17	1.17	1.16	2.06	2.06	2.05	7.13	7.11	7.08
-100 MPa	FeSi NO	19.86	19.81	19.72	51.18	51.04	50.81	4.97	4.95	4.93	0.50	0.50	0.49
-100 MPa	FeSi GO	62.78	62.60	62.32	15.75	15.70	15.63	1.57	1.57	1.56	0.16	0.16	0.16
-100 MPa	Fe-amorph	51.08	50.93	50.70	53.20	53.05	52.81	5.32	5.31	5.28	0.53	0.53	0.53
-100 MPa	Terfenol-D	13.83	13.79	13.73	1.17	1.17	1.16	2.06	2.06	2.05	7.13	7.11	7.08

Table A.4: Ratio r for different current I and stress σ levels for a selection of magnetostrictive materials. A light color indicates a ratio $r > 5$ and a dark color indicates $r > 25$.

Finally, to assess the practicality of energy harvesting from Ericsson cycles, the question of the electrical converter has to be considered. A possibility is to consider a bidirectional DC-DC converter. Based the energy densities reported in Table 2 and with the considered geometry, electrical powers in the range of [1 250] W at f = 50 Hz are expected. For such powers, commercially available DC-DC converters such as MAX797 [21] or MAX1653 [22] exhibit up to 96% efficiency. A rough estimation can be obtained for the voltage amplitude based on (A.4), where S is the rod cross-section, ω the angular velocity, and ΔB the maximal variation of the magnetic induction along with the Ericsson cycle.

$$V = n\, S\, \omega\, \Delta B \tag{A.4}$$

A few volts are obtained in the low field range and up to more than 1000 V in the extreme case of the Terfenol-D for H_m = 100 kA.m^{-1} and N = 20 000 turns. Besides this extreme case, all colored cells in Table A.4 lead to reasonable values, low enough to be used as input of the proposed DC-DC converters.

References

[1] N. Panayanthatta, G. Clementi, M. Ouhabaz, M. Costanza, S. Margueron, A. Bartasyte, S. Basrour, E. Bano, L. Montes, C. Dehollain, R. La Rosa, "A Self-Powered and Battery-Free Vibrational Energy to Time Converter for Wireless Vibration Monitoring", *Sensors*, **21(22)**:7503, 2021.

[2] S. Zeadally, F.K. Shaikh, A. Talpur, Q.Z. Sheng, "Design architectures for energy harvesting in the Internet of Things", *Renewable and Sustainable Energy Reviews*, **128**:109901, 2020.

[3] P. Kamalinejad, C. Mahapatra, Z. Sheng, S. Mirabbasi, V.C. Leung, Y.L. Guan, "Wireless energy harvesting for the Internet of Things", *IEEE Communications Magazine*, **53(6)**:102-108, 2015.
[4] K. Veni Selvan, M. S. M. Ali, "Micro-scale energy harvesting devices: Review of methodological", *Renewable and Sustainable Energy Reviews*, **54**: 1035-1047, 2016.
[5] J. Krikke, "Sunrise for energy harvesting products", *IEEE Pervasive Computing*, **4(1)**:4-5, 2005.
[6] Z. Deng, M.J. Dapino, "Review of magnetostrictive vibration energy harvesters", *Smart Materials and Structures*, **26(10)**:103001, 2017.
[7] G. Backman, B. Lawton, N.A. Morley, "Magnetostrictive energy harvesting: Materials and design study", *IEEE Transactions on Magnetics*, **55(7)**:1-6, 2019.
[8] J. Hu, F. Xu, A.Q. Huang, F.G. Yuan, "Optimal design of a vibration-based energy harvester using magnetostrictive material (MsM)", *Smart materials and structures*, **20(1)**:015021, 2010.
[9] A. Viola, V. Franzitta, G. Cipriani, V. Di Dio, F.M. Raimondi, M. Trapanese, "A magnetostrictive electric power generator for energy harvesting from traffic: Design and experimental verification", *IEEE Transactions on Magnetics*, **51(11)**: 1-4, 2015.
[10] S.P. Beeby, T. O'Donnell, "Electromagnetic energy harvesting", *In: S. Priya, D.J. Inman (eds) Energy Harvesting Technologies*, Springer, Boston, 2009.
[11] F.U. Khan, M.U. Qadir, "State-of-the-art in vibration-based electrostatic energy harvesting", *Journal of Micromechanics and Microengineering*, **26(10)**:103001, 2016.
[12] H. Liu, J. Zhong, C. Lee, S.W. Lee, L. Lin, "A comprehensive review on piezoelectric energy harvesting technology: Materials, mechanisms, and applications", *Applied Physics Reviews*, **5(4)**:041306, 2018.
[13] A. Sisman, H. Saygin, "On the power cycles working with ideal quantum gases: I. The Ericsson cycle", *Journal of Physics D: Applied Physics*, **32(6)**:664, 1999.
[14] Y. Liu, B. Ducharne, G. Sebald, K. Makihara, M. Lallart, "Investigation of Energy Harvesting Capabilities of Metglas 2605SA1", *Applied Sciences*, **13(6)**:3477. 2023.
[15] L. Daniel, "An analytical model for the effect of multiaxial stress on the magnetic susceptibility of ferromagnetic materials", *IEEE Transactions on Magnetics*, **49(5)**:2037-2040, 2013.
[16] L. Daniel, M. Domenjoud, "Anhysteretic magneto-elastic behaviour of Terfenol-D: experiments, multiscale modelling and analytical formulas", *Materials*, **14(18)**: 5165, 2021.
[17] F. Fiorillo, "Magnetic materials for electrical applications: a review", *INRIM Technical Report 13/2010*, 2010.
[18] M. Domenjoud, E. Berthelot, N. Galopin, R. Corcolle, Y. Bernard, L. Daniel, "Characterization of Giant Magnetostrictive Materials under static stress: influence of loading boundary conditions", *Smart Materials and Structures*, **28(9)**: 095012, 2019.
[19] M. Domenjoud, A. Pécheux, L. Daniel, "Characterization and multiscale modeling of the magneto-elastic behavior of Galfenol", *IEEE Transactions on Magnetics*, 2023 (doi.org/10.1109/TMAG.2023.3280925).
[20] M. Zucca, M. Hadadian, O. Bottauscio, "Quantities affecting the behavior of vibrational magnetostrictive transducers", *IEEE Transactions on Magnetics*, **51(1)**: 8000104, 2015.
[21] Step-Down Controllers with synchronous Rectifier for CPU Power, MAX797, ANALOG DEVICES. [Online]. Available: https://www.analog.com/en/products/max797.html#product-overview
[22] High-Efficiency, PWM, Step-Down DC-DC Controllers in 16-Pin QSOP, MAX1653, ANALOG DEVICES. [Online]. Available: https://www.analog.com/en/products/max1653.html#product-overview